

Assessment of an Active Electromagnetic Sensor for Hunting Buried Naval Mines, Part II

P.J. Carroll, W.M. Wynn, and J.W. Purpura
Naval Surface Warfare Center
110 Vernon Avenue
Panama City, FL 32407 USA
paul.carroll@navy.mil

Abstract — The US Navy is investigating the use of broadband electromagnetic (EM) sensors as a candidate technology for its Buried Minehunting (BMH) sensor suite. New Navy tactics are being pursued, where short-range sensors are incorporated into reacquisition minehunting systems for short-range classification. The current approach includes study of use of active EM sensors that employ multi-frequency sources for target illumination which can provide valuable multi-spectral discrimination for the classification of buried naval mines.

In 2004, the Navy evaluated the detection/classification performance of a Geophex, Ltd. GEM3 sensor by performing underwater tests versus selected ideal targets and simulated mine targets. Test results demonstrated that GEM3 can detect metallic ordnance buried in the ground and under the sea bottom at short ranges. GEM3 tests demonstrated that electromagnetic induction spectroscopy (EMIS) techniques could be used to measure the spectral “fingerprint” of a target, which assists in target identification. FY04 GEM3 tests also showed that the active EM detection range must be increased if these sensors are to be a useful identification sensor in an autonomous underwater vehicle (AUV) reacquisition system.

In this paper, we report results measuring the performance of a new Geophex active EM sensor that employs new coil configurations designed to extend the detection range and increase background noise rejection. The new coil configuration which contains multiple active EM sensors is designed at a comparable size with the 12 ¾” AUVs that the BMH program is developing for its reacquisition minehunting systems. Results from rail experiments with the new sensor operating on land are described.

I. INTRODUCTION

The U.S. Navy has been investigating the use of active broadband EM sensors as a candidate for its Buried Minehunting (BMH) sensor suite [1]. The approach being taken under the BMH project divides the minehunting mission into a two-phase operation where long-range active sonars and shorter ranged sonar and EM sensors are operated from small AUVs in a cooperative mode to detect and identify mine targets. In the search-classify-map (SCM) operation, long range active sonar in one AUV identifies mine-like objects and passes an objects position information to a second AUV which

uses a suite of short-range sensors to perform the reacquisition and identification (RI) operation. When the mine-like targets are buried in the sea bottom, the identification task is challenging requiring multiple sensors to obtain sufficient target information to permit identification.

Previous tests conducted by Geophex, Ltd and the Naval Surface Warfare Center, Panama City, Florida have demonstrated that active broadband EM sensors provide a much greater amount of information about a target than can be obtained by passive magnetic sensors. An active EM sensor transmits an EM signal that interacts with a metallic target generating eddy currents that produce a secondary EM field response sensed by a receiver coil of the sensor. The target’s response largely depends on the object’s size, shape, orientation, depth, electrical conductivity, and magnetic permeability. Operating the active EM sensor at several frequencies, EM induction spectroscopy (EMIS) techniques were used to demonstrate measurement of the spectral “fingerprint” of several different targets.

The results of the 2004 Navy assessment of the performance of a Geophex GEM3 sensor in detecting and identifying underwater buried mine targets was reported in a previous OCEANS proceeding [2]. The results were encouraging but several challenges remained which are addressed in a Phase II sensor development and test project during 2005 and 2006. In Phase II NSWC-PC and Geophex developed a new active EM sensor, designated the GEM53D sensor, which is designed to be configured for operation onboard a 12 ¾” diameter AUV, operate with greater sensitivity to increase the sensor range, and include ancillary sensors to permit application of ambient noise rejection techniques. The GEM53D is designed for operation and testing in a series of land and underwater tests to demonstrate its detection and identification capability and characterization of limiting sensor and environmental noise factors. NSWC-PC developed sensor and environmental models to assist in the assessment of performance and to identify sensor and environmental sources limiting sensor performance in the underwater environment.

This paper reports on the development and analysis of the GEM53D sensor performance during initial land tests conducted primarily in NSWC-PC’s Nonmagnetic Test Facility. Section II includes a description of the GEM53D sensor including ancillary sensors. Section III describes the experimental setup, including the specialty test equipment developed for sensor calibration and in-motion operation.

This work was sponsored by the U.S. Office of Naval Research. The appearance of trade names in this document does not constitute endorsement by the Department of Defense; the United States Navy; or the Naval Surface Warfare Center.

Report Documentation Page

Form Approved
OMB No. 0704-0188

Public reporting burden for the collection of information is estimated to average 1 hour per response, including the time for reviewing instructions, searching existing data sources, gathering and maintaining the data needed, and completing and reviewing the collection of information. Send comments regarding this burden estimate or any other aspect of this collection of information, including suggestions for reducing this burden, to Washington Headquarters Services, Directorate for Information Operations and Reports, 1215 Jefferson Davis Highway, Suite 1204, Arlington VA 22202-4302. Respondents should be aware that notwithstanding any other provision of law, no person shall be subject to a penalty for failing to comply with a collection of information if it does not display a currently valid OMB control number.

1. REPORT DATE 01 SEP 2006	2. REPORT TYPE N/A	3. DATES COVERED -	
4. TITLE AND SUBTITLE Assessment of an Active Electromagnetic Sensor for Hunting Buried Naval Mines, Part II		5a. CONTRACT NUMBER	
		5b. GRANT NUMBER	
		5c. PROGRAM ELEMENT NUMBER	
6. AUTHOR(S)		5d. PROJECT NUMBER	
		5e. TASK NUMBER	
		5f. WORK UNIT NUMBER	
7. PERFORMING ORGANIZATION NAME(S) AND ADDRESS(ES) Naval Surface Warfare Center 110 Vernon Avenue Panama City, FL 32407 USA		8. PERFORMING ORGANIZATION REPORT NUMBER	
9. SPONSORING/MONITORING AGENCY NAME(S) AND ADDRESS(ES)		10. SPONSOR/MONITOR'S ACRONYM(S)	
		11. SPONSOR/MONITOR'S REPORT NUMBER(S)	
12. DISTRIBUTION/AVAILABILITY STATEMENT Approved for public release, distribution unlimited			
13. SUPPLEMENTARY NOTES See also ADM002006. Proceedings of the MTS/IEEE OCEANS 2006 Boston Conference and Exhibition Held in Boston, Massachusetts on September 15-21, 2006, The original document contains color images.			
14. ABSTRACT			
15. SUBJECT TERMS			
16. SECURITY CLASSIFICATION OF:			17. LIMITATION OF ABSTRACT
a. REPORT unclassified	b. ABSTRACT unclassified	c. THIS PAGE unclassified	UU
			18. NUMBER OF PAGES 8
			19a. NAME OF RESPONSIBLE PERSON

Section IV describes the GEM53D model developed by NSWC-PC which has been used in the sensor performance evaluation. Section V describes results of GEM53D stationary and in-motion performance results and compares the results with modeling results. Section VI lists the conclusions based on tests/analysis to date and outlines the plans for future testing of GEM53D underwater versus selected targets.

II. GEM53D SENSOR

The GEM53D consists of a GEM5 gradiometer and a GEM3 with tri-axial receiver coils, known as GEM3D, as depicted in Fig. 1. The GEM53D structure also includes three sets of orthogonal electrode pair probes which serve as ancillary sensors measuring electric fields in the GEM5 sensor area and are used for environmental noise cancellation. All sensors are mounted on a monolithic cylindrical structure carved out of 12-inch schedule 80 polyvinyl chloride (PVC) pipe that has a wall thickness of about 0.4 inches. The two active EM sensors share common transmitter coils. The GEM53D design includes several features to enhance sensor sensitivity and reject background environmental noise and is designed with a configuration and size consistent with a 12 3/4" AUV. GEM 5, the primary active EM sensor, is configured for gradient operation to reject coherent background noise. GEM3D is designed to characterize the individual field components and permit investigation of use of field components in potential noise rejection techniques. Design features have been incorporated to extend the range of the GEM sensors, including increasing the transmission coil voltage (increased moment) by a factor of two and use of 24 bit analog-to-digital converters. In addition, GEM53D will employ processing techniques including detector functions which average sensor outputs at multiple frequencies to enhance the target signal to noise. GEM53D is intended to be a prototype which will assist in determining the final active EM sensor geometry and configuration for the forthcoming BMH vehicle.

Fig. 2 shows the GEM53D sensor as constructed. All coils, wiring and embedded preamp electronics are waterproofed

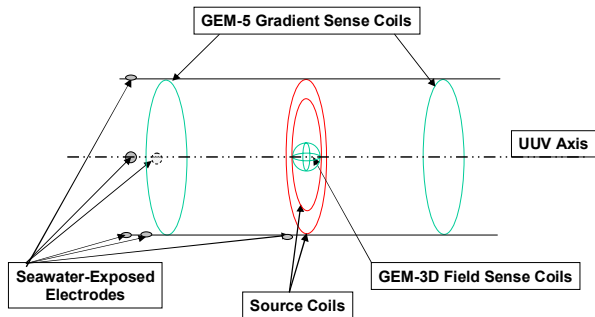


Figure 1. GEM53D Sensor Configuration

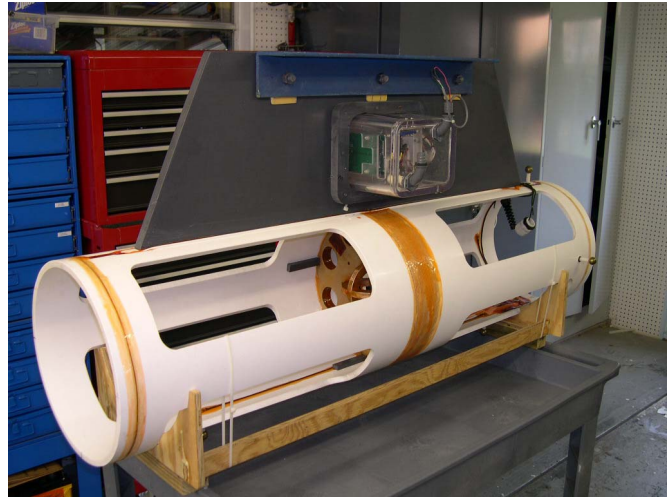


Figure 2. GEM53D Sensor and Electronics with Support Fin./Clamp

using a polyurethane coating. Seven channels of GEM53D processing and the transmitter power electronics are housed in the plastic waterproof box attached to the support fin. The plastic support fin is used to connect GEM53D to the rail pendant (described below) during sensor motion tests. The GEM3 receive coils are mounted via a bulkhead internal to the cylinder.

III. EXPERIMENTAL SETUP

We conducted experiments with the GEM53D active electromagnetic sensor operating in air to obtain an initial characterization of its performance prior to any underwater testing. This land-based testing allowed us to check out the sensor more conveniently under controlled conditions than possible when working with the sensor submerged underwater. In order to accurately compare our model predictions with our experimental results, we performed a series of careful measurements of sensor response to a 12-inch-diameter hollow stainless steel (SS) spherical target placed at precisely known positions. We also measured the stationary noise of the sensor in air and made measurements of the sensor response as it was moved past our stationary spherical target.

Our experiments were performed in the 10-acre nonmagnetic test range of our Panama City, Florida facilities, which is a controlled-access area established for testing a wide variety of magnetic sensors. To facilitate precise, repeatable positioning of the target sphere with respect to the sensor, we built two identical saw-horse-like structures out of pressure-treated lumber to support vertical posts containing horizontal pegs spaced every 15 centimeters (6-inches) from top to bottom (see Fig. 3). The saw-horse structures were separated by approximately 3.5 meters as shown and 1.8-meter-long horizontal cross members were placed across the pegs to support a 4.25-meter-long wooden beam used to hold the target sphere at an adjustable height. A series of 10-centimeter-diameter (4-inch) counter bores were drilled into the top surface of the target beam along its full length, with 15-centimeter (6-inch) spacing, to provide a repeatable means of placing the 12-inch spherical shell in position.

We placed the GEM53D sensor on a wooden table between the saw-horse structures and leveled its primary cylindrical axis approximately 1.2 meters above the ground. Care was taken during the initial setup to align and level the target support structures such that the target beam was parallel to the sensor axis and the cross members were orthogonal to the beam. Our experimental setup was designed to allow the target beam to be moved in precise increments side-to-side as well as vertically, while maintaining parallel alignment with the sensor. Using this apparatus, we estimate our target positions measured with respect to the center of the sensor were accurate to within one centimeter, and repeatable to within a couple of millimeters.

The static measurements of sensor response to the stainless steel shell, taken to test our model predictions, were obtained for each discrete position along the target beam. Measurements of this type were recorded for several lateral and vertical offsets of the beam.

For our measurements of sensor response while it moved past a stationary target, we modified the design of the sensor-translation apparatus used in our earlier work [2] to accommodate the larger size of the GEM53D and to incorporate some general improvements. The redesigned apparatus, consisting of two tall support towers bridged by an

overhead rail transited by a trolley carrying the sensor holder, is shown in Fig. 3. The height of each of the three-legged PVC towers was extended by approximately one meter from the original design, making them 5.6 meters tall. This additional height will allow the apparatus to be set up in deeper water to provide the sensor additional standoff distance from the sea bottom and the water surface. The rail is comprised of dual 9.75-meter-long fiberglass I-beams attached together to make it highly resistant to twist, in contrast to the single I-beam design we used in our earlier investigation. This feature will provide greater control of our sensor path when we operate in the tidal currents and choppy waves generally present in our bay waters.

The trolley is designed to hug the rail with upper and lower rollers riding on the top and bottom surfaces of the I-beam pair, respectively. The upper segment of the sensor holder consists of four vertical 10-foot lengths of nominal 4-inch diameter PVC pipe that pass through guide bushings and clamps on the sides of the trolley to set the sensor height. The sensor attaches to the lower segment of the holder with fiberglass bolts. Ropes attached to the trolley were used to manually pull the sensor along the rail when performing motion tests.



Figure 3. Experimental apparatus used for static and in-motion measurements in our investigation of the GEM53D active electromagnetic sensor.

IV. GEM53D MODEL

The GEM53D sensor described above (see Fig. 1) is geometrically more complicated than the GEM3 sensor described in previous work [2]. There are two additional sense axes at the primary-bucking coil center (GEM3Y and GEM3Z), and two new coils physically displaced along the axis of the primary (GEM5 fore and aft). These two coils are differenced to produce the GEM5 signal. An additional operational difference between the GEM53D and the GEM3 has to do with axial orientation of the primary coil at the Closest Point of Approach (CPA) of the target. With the GEM3, the primary coil *axis* passes through the target at CPA, whereas with the GEM53D, the *plane* of the primary coil will pass through the target at CPA. This change is driven by the requirement that the GEM53D configuration be compatible with the geometry of an AUV. Physically, this leads to some reduction in signal. With the GEM53D, the primary field at the target will be roughly half the magnitude that would occur for the GEM3 configuration. In turn, the scattered field seen by GEM3X at CPA will be roughly half that for the GEM3 configuration. Thus, the overall signal return is reduced by roughly a factor of 4 relative to a GEM3 configuration with the same source and sensor coil parameters.

The procedure for modeling the target signals for the GEM53D is an extension of the method used for the GEM3, which was reported in a previous paper [2]. The underlying model is that of scattering time-harmonic dipole source fields from a spherical shell of arbitrary composition, with the shell imbedded in a uniform medium of arbitrary composition (typically air or seawater) [3]. The solution for the elemental current dipole is the tool (basic Green function) used for the synthesis of the sensor model. The source and bucking coils are divided into small segments, with each segment approximated by a current dipole vector of appropriate strength and orientation. The sense coils are divided into segments of appropriate length and orientation, and the scattered electric field is computed at the center of each segment. The resulting values are used to approximate a line integral of the electric field around the sense coil periphery, producing an induced voltage. The resulting voltages are then scaled by the voltage induced by the primary coil in the GEM3X sense coil (GEM3D signals), or by the voltage induced by the primary coil in one of the axially-displaced

GEM5 coils (GEM5 signal), to produce the Geophex Parts-Per-Million (PPM) simulated output.

For comparison, we show the GEM53D and GEM3 system parameters in Table 1. We will give some model results in the following section.

V. EXPERIMENT AND RESULTS

A. Controlled Experiments in Air: Comparison to GEM53D Model

The first experiment involved the placement of a stainless steel shell at precise positions relative to the stationary GEM53D sensor, as described in Section III, and measuring the response at multiple frequencies. For each position of the target we took a brief record with no target present followed by a record with the target present. The sensor outputs were then averaged over the duration of the record with target present (~5 seconds at a 30-hertz sample rate). In this fashion we compiled a database of sensor responses for a variety of precisely known sensor-target relative positions. The frequencies used (all odd multiples of 30 hertz) were 90, 210, 390, 750, 1470, 2910, 5850, 11430, and 21690 hertz. Two sensor locations relative to the target are shown in end view in Fig. 4. The motion of the sensor relative to the target is into the plane of the page. The positions along track ranged from -1.525 m to 1.667 m for the closest pass, and -1.981 m to 1.981 m for the outer run. In the runs, the increment in x was 0.152 m. For the shell, we used a diameter of 11.5 inches, thickness 12 gauge, electrical conductivity 1.4×10^6 S/m, and a relative permeability of 1.035.

For the various runs, the measurement-model match is very good at all frequencies for the GEM3X channel. For the GEM5 channel, the comparisons are good below 5850 hertz, with severe drift and quantization noise seen in the GEM5 measured data at higher frequencies. We will have more to say about this below. We show results for GEM3X and GEM5 for the three frequencies (390, 750 and 1470 hertz) spanning the range where the in-phase and quadrature responses exchange dominance (the crossover frequency is 750 hertz). We show results for the 0.344 m lateral separation in Fig. 5. This result is a rigorous test of the total model, because of the close proximity of the target to the coils. We show the results for the 0.701 m lateral separation in Fig. 6.

TABLE 1

GEM53D AND GEM3 SYSTEM PARAMETERS

GEM53D	GEM3
Primary Coil: $r = 0.1610\text{m}$, $N = 18$ (X-oriented) Bucking Coil: $r = 0.0816\text{m}$, $N = 8$ (X-oriented)	Primary Coil: $r = 0.20\text{m}$, $N = 12$ (Z-oriented) Bucking Coil: $r = 0.11074\text{m}$, $N = 8$
3X Coil: $r = 0.050\text{m}$, $N = 100$ 3Y Coil: $r = 0.050\text{m}$, $N = 100$ 3Z Coil: $r = 0.050\text{m}$, $N = 100$	3Z Coil: $r = 0.0625\text{m}$, $N = 100$
5X forward Coil: $r = 0.1610\text{m}$, $N = 100$ 5X aft Coil: $r = 0.1610\text{m}$, $N = 100$	
5X fore-aft spacing: $d = 1.219\text{m}$	

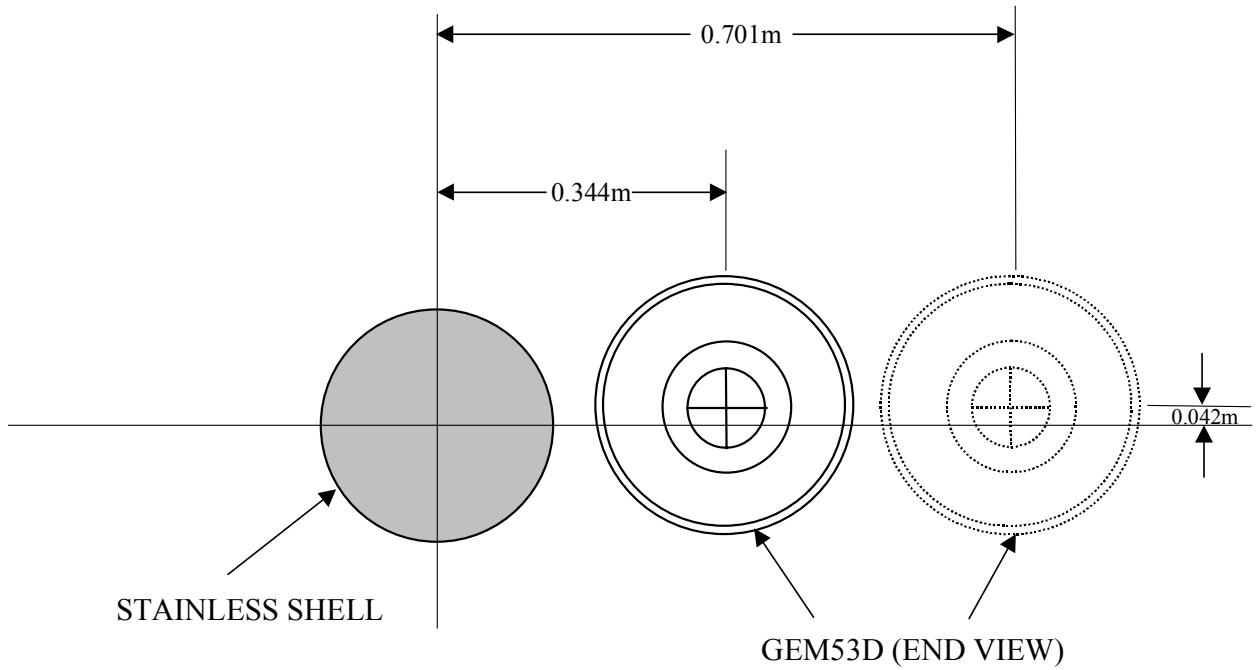


Figure 4. Geometry for precision measurement-model testing GEM53D runs.

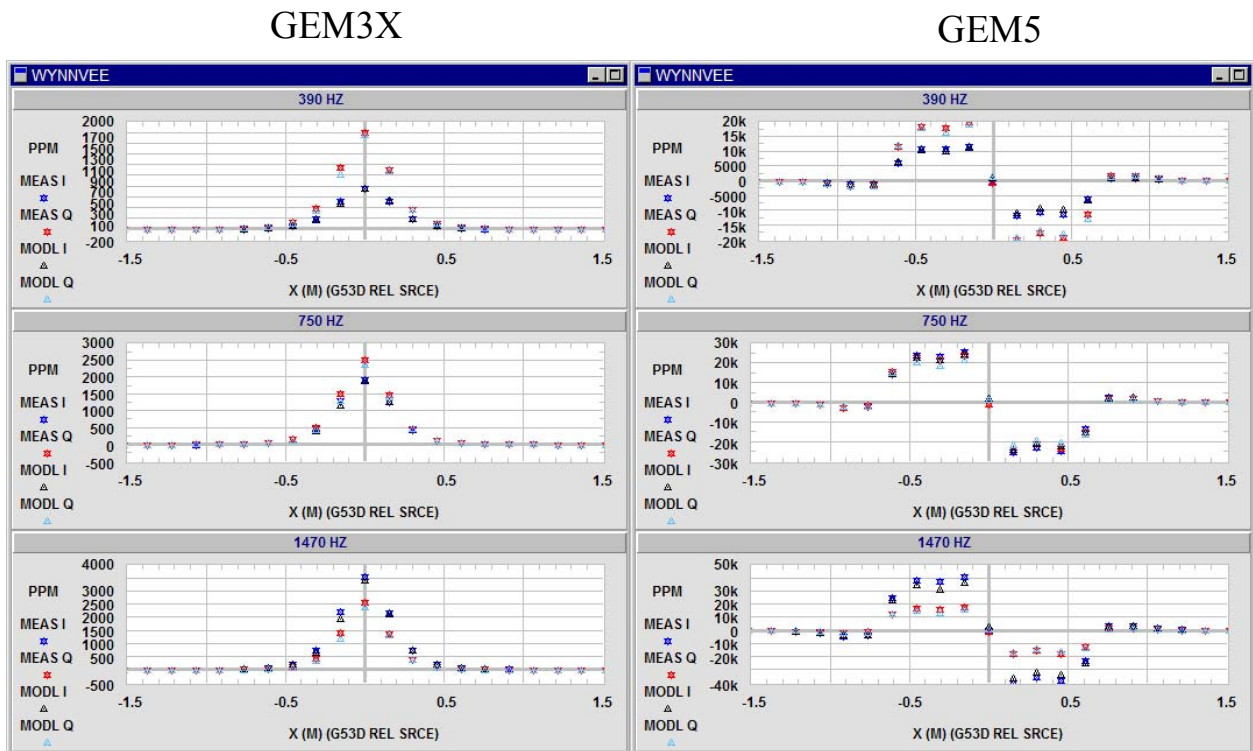


Figure 5. GEM3X and GEM5 measured and modeled response at 0.344 m.

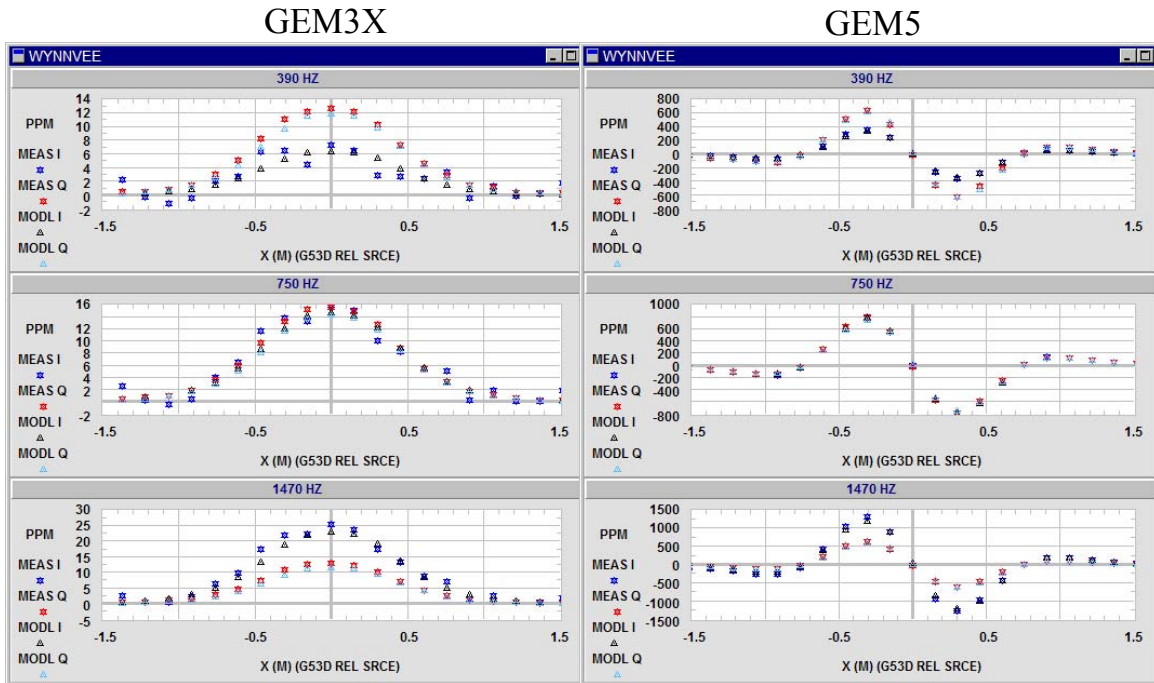


Figure 6. GEM3X and GEM5 measured and modeled response at 0.701 m

B. Stationary Noise Measurements

To characterize the low-frequency drift of the multi-frequency signal levels of GEM53D, we performed extended noise runs in a quiet area, with the sensor supported away from the ground. The runs were 10 minutes long. Data for each frequency was sampled at 30 hertz. All of the GEM53D channels show significant drift in time for all of the selected frequencies. The source of this drift is not yet understood. Part of the drift may be due to background power fields leaking into the measurement, and there is almost certainly a thermal contribution. The measurements were made in sunlight with wind blowing over the sensor. This issue is being revisited, and more measurements will be done when the GEM53D is sealed and placed in a seawater environment.

The sense channel that will ultimately be used in AUV applications is almost certainly the GEM5. This choice is driven by physical configuration constraints, as well as the robustness of the signal. As mentioned above, the GEM5 was noisy at the higher frequencies, but performed well below 5850 hertz. For illustration, we show the stationary noise behavior for the GEM5 for the 1470-hertz line. In Fig. 7, we show both the time history and the associated amplitude spectrum of the noise for both I and Q signals. The spectra were computed using a sine window with 265 samples and 50% overlap. The choice of 256 samples corresponds to roughly an eight-second window at the 30 hertz sample rate. An eight second window spans approximately 12 meters for a AUV moving at the typical speed of three knots. This is more than enough to encompass the complete signal trace from targets detectable by the GEM 5. As we will see below, the use of a 12-meter window may be optimistic.

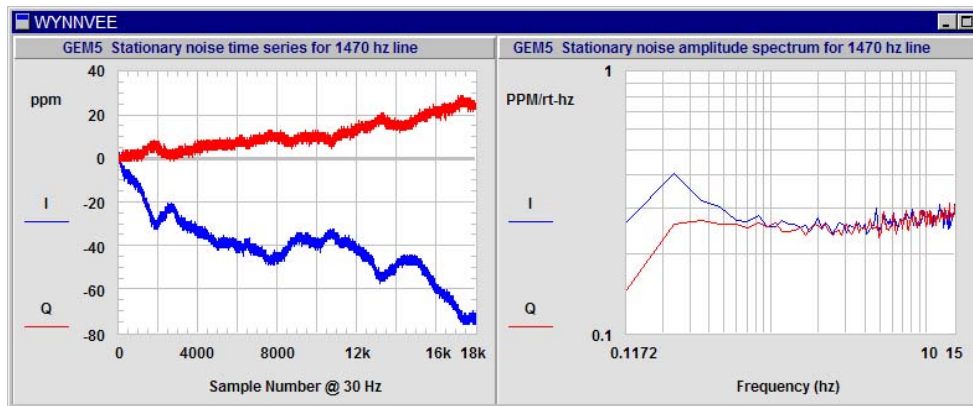


Figure 7. GEM5 1470-hertz stationary noise (time and frequency).

C. Target Range Measurements: GEM53D in Motion

To get a sense of the performance of the GEM53D in motion, we rearranged the target-positioning matrix, as described in Section III, and placed the stainless steel shell target at various lateral CPA distances from the path of the sensor. The axis of the GEM53D was placed 0.51 m above a plane passing through the center of the target. The sensor was then manually translated along the supporting rail for a distance of $\sim\pm 5$ m from CPA. The results are shown in Fig. 8. The ranges shown are the slant ranges (total distance at CPA). From the figure, we see that the presence of the target is discernable by eye out to a range of ~ 1.5 meters. The signal decreases rapidly with range ($\sim r^{-6}$ for the GEM3, $\sim r^{-6+}$ for the GEM5). There appears to be a possible bias in the signal associated with the local environment, but this is not definite.

D. Detection Range: Signal Energy Compared to Stationary Noise

The previous data raises the question as to what the maximum detection range is for the GEM5 against a 12-inch target. To address this question, we invoke the scattering

model described above to calculate the GEM5 signals at 0.1-m increments in x for various CPA ranges. These signals are then splined to emulate the 30-hertz sample rate, and the target signal energy as a function of frequency is calculated by fourier transforming the signal and computing the squared modulus. The noise power spectrum is obtained by squaring the amplitude spectrum shown in Fig. 7. The signal energies and noise power are shown in Fig. 9. We note that the matched-filter signal-to-noise ratio is computed as the frequency integral of the ratio of the signal energy to the noise power. Inspection of Fig. 9 suggests that the target is detectable out to a lateral range of 2.25 m, if the stationary noise can be achieved in motion. This is a major challenge for the application of this sensor to detection.

VI. CONCLUSION AND FUTURE WORK

We have performed an initial assessment of an active EM sensor prototype, the GEM53D, designed in an AUV-compatible configuration for use as a buried sea mine reacquisition and identification sensor. We have measured the GEM53D stationary noise characteristics and the EM response of a spherical metallic target during land tests where

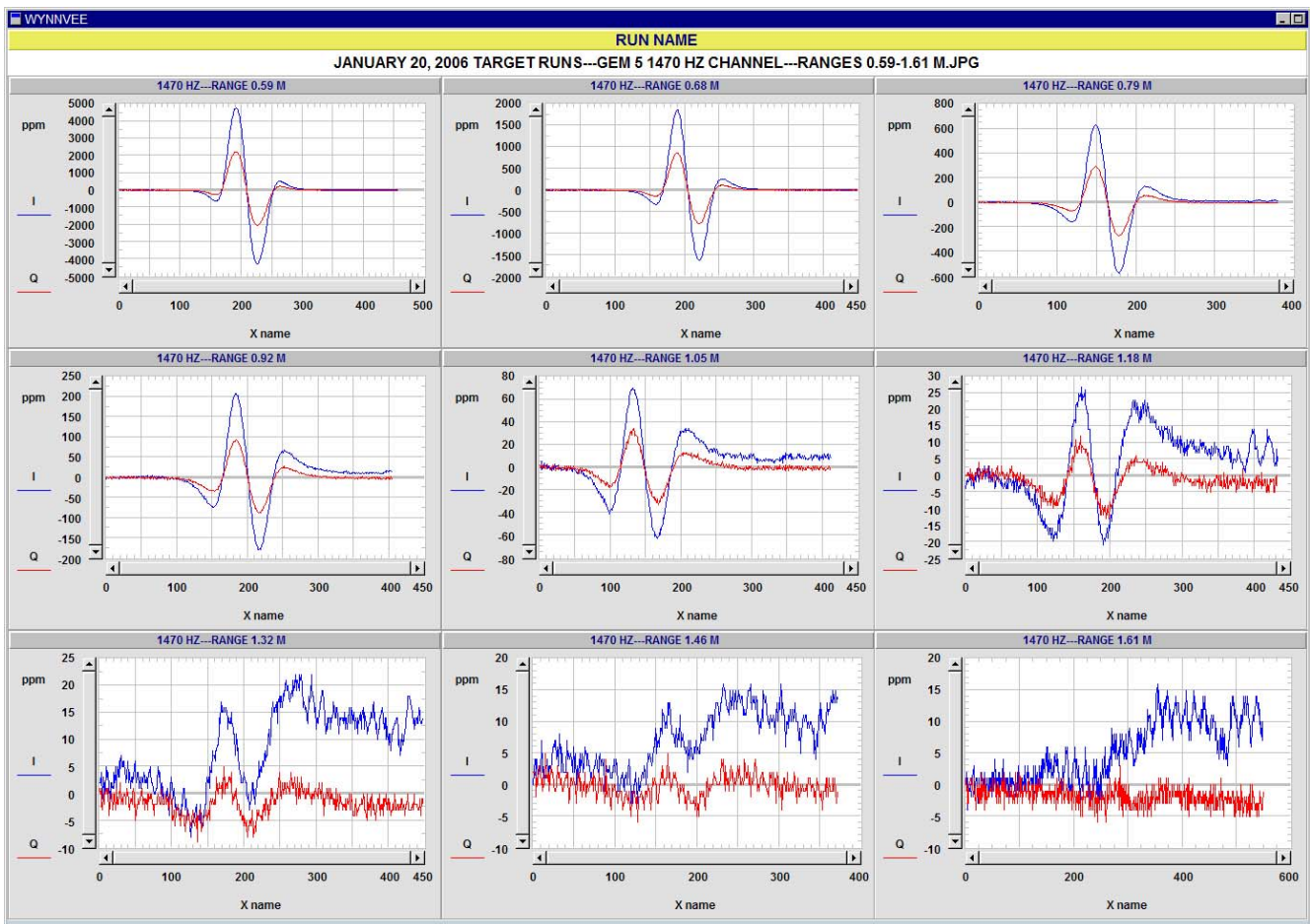


Figure 8. GEM5 in motion: target signatures at various ranges.

GEM 5 SIGNAL ENERGY AND NOISE POWER SPECTRA---12 INCH SS SHELL (VERTICAL OFFSET 0.5 M---LABELS ARE LATERAL RANGE)

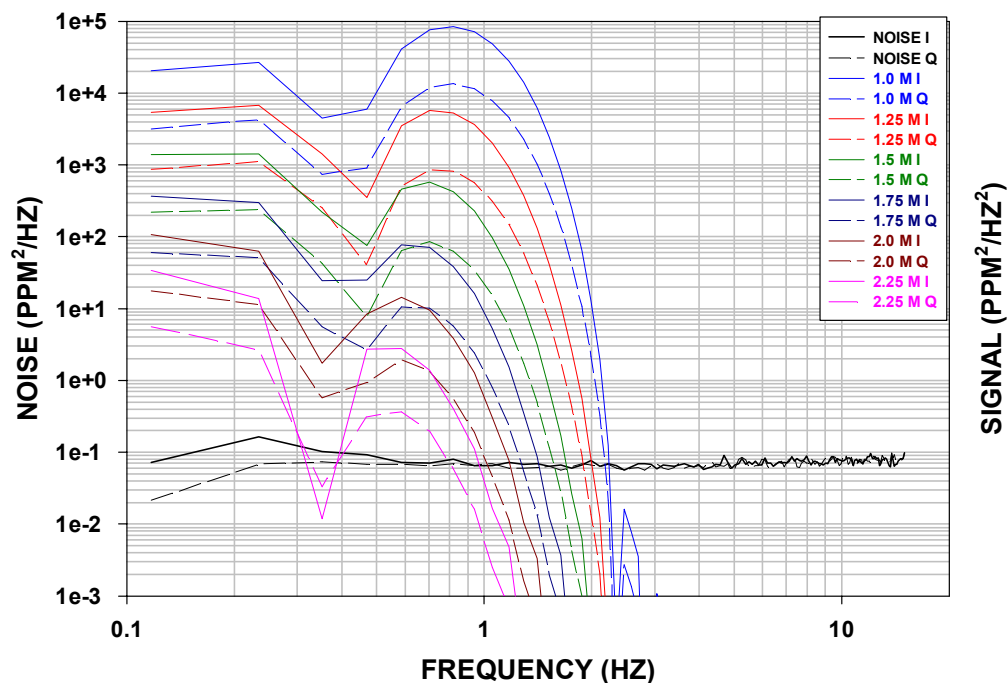


Figure 9. Target signal energy at various ranges compared to stationary sensor noise.

the GEM53D was translated past the target in a controlled manner. We have also incorporated the GEM53D sensor geometry into a model to compute the response of spherical targets suspended in an unbounded conducting or non-conducting medium to an active EM source. Our model predictions agree with our measured results to within the limits of our experimental error.

Measurements of GEM53D target detection range were made translating the GEM53D sensor past a 12" stainless steel spherical target at various lateral CPA distances. The presence of the target was discernable by eye in the GEM5 response out to ranges of ~ 1.5 meters at frequencies lower than 5KHz. The maximum detection range of the 12" target was estimated by calculating a matched-filter signal-to-noise ratio using the GEM5 model, and measured GEM5 stationary noise amplitude spectra. The GEM5 signal energy for the target at various lateral distances suggests that the target is detectable to 2.25meters if GEM5 stationary noise can be achieved in motion underwater. This is the key challenge to achieving target identification at useful BMH ranges.

The GEM53D sensor is currently undergoing modification to seal all sensor coils and electronics for underwater operation. Preliminary tests performed on GEM53D indicate that the sensor noise drifts with temperature change in the electronics area. Modifications have been made to the GEM53D electronic housing to air cool and stabilize the temperature of sensor electronics for future land and underwater operation.

GEM53D tests are scheduled in late summer 2006 to demonstrate the underwater detection capability of GEM53D and to characterize limiting sensor and environmental noise sources. The underwater test results will provide guidance for development of a BMH GEM sensor compatible with a 12 $\frac{3}{4}$ " AUV which will be used in U.S. Navy BMH sea tests.

ACKNOWLEDGMENT

The authors gratefully acknowledge the support of Dr. Kerry Commander (ONR321MS) who made this work possible. We are grateful to I.J. Won, Alex Oren, and Bill SanFilipo, all of Geophex, Ltd., for development of the GEM53D sensor and their assistance in this work. We also thank Mark Scheer, of NSWC-PC, for valuable support during our measurements.

REFERENCES

- [1] T. Clem, "Sensor technologies for hunting buried sea mines," *MTS/IEEE Oceans 2002*, pp. 452-460, 2002.
- [2] J.W. Purpura, W.M. Wynn, and P.J. Carroll, "Assessment of an Active Electromagnetic Sensor for Hunting Buried Naval Mines," *MTS/IEEE Techno-Oceans '04*, pp. 879-889, 2004.
- [3] W.M. Wynn, "Electromagnetic fields of a uniform sphere in a uniform conducting medium with application to dipole sources," Technical Report NCSC TR 426-90, September 1991.